Mol Biol Rep (2012) 39:7389–7402
DOI 10.1007/s11033-012-1571-6

Cell cycle arrest and apoptosis by expression of a novel TPIP (TPIP-C2) cDNA encoding a C2-domain in HEK-293 cells

Rasmi Rekha Mishra · Jitendra Kumar Chaudhary · Pramod C. Rath

Received: 24 May 2011 / Accepted: 25 January 2012 / Published online: 7 February 2012

Abstract The human TPIP (TPTE and PTEN homologous Inositol lipid Phosphatase) belongs to the PTEN (Phosphatase and TENsin homologue deleted on chromosome 10) family of dual-specific phosphatases and is expressed from the human chromosome 13 as multiple splice-variants, e.g., TPIPα, β, γ mRNAs. PTEN is a well characterized tumor suppressor, which controls survival, adhesion, motility and migration of mammalian cells, its C2-domain plays crucial role in controlling these functions. However, role of isolated C2-domain protein in regulation of cell proliferation and apoptosis is not reported. We report sequence analysis and function of a novel human TPIP (TPIP-C2) cDNA encoding a 193 amino acid C2-domain in cell proliferation and apoptosis regulation. In silico analysis and homology modelling revealed that the C2-domain of TPIP-C2 is similar to that of PTEN but with short disorder sequences overlapping or adjacent to the post-translational modification sites. Overexpression of TPIP-C2 cDNA in human embryonic kidney (HEK-293) cells caused cell cycle arrest, inhibition of cell proliferation and induced apoptosis in an activated caspase 3 and PARP-dependent manner in comparison to overexpression of the full length human PTEN cDNA. TPIP-C2 overexpressed cells also showed S-phase cell cycle arrest. We suggest that C2-domain of TPIP-C2 may act as a dominant negative effector, which may bind to and arrest the cell proliferation signalling complex and isolated TPIP-C2-domain-like proteins expressed in mammalian cells/tissues may play important role in regulation of cell proliferation and apoptosis. The TPIP-C2 cDNA may be exploited for inducing cell cycle-inhibition and apoptosis in human cancer cells and tissues.

Keywords TPIP · C2-domain · Cell proliferation · Apoptosis

Electronic supplementary material The online version of this article (doi:10.1007/s11033-012-1571-6) contains supplementary material, which is available to authorized users.

R. R. Mishra · J. K. Chaudhary · P. C. Rath (✉)
Molecular Biology Laboratory, School of Life Sciences, Jawaharlal Nehru University, New Delhi 110067, India
e-mail: pcrath@mail.jnu.ac.in

Introduction

Mammalian cells universally depend on interaction of extracellular matrix (ECM), cell surface associated proteins and cytoskeleton to initiate and promote cell growth and proliferation. This interaction is partly controlled by protein phosphorylation, which is a well characterized reversible post-translational modification that regulates protein activity by protein kinases and protein phosphatases. This event is under tight control to maintain homeostasis of cellular growth, proliferation and apoptosis. Any aberrant activity of such protein kinases and phosphatases may lead to cellular imbalance and give rise to complex disorders like cancer [1]. In human genome, the total number of known kinases and phosphatases are 501 and 100, respectively. Out of these, there are only 29 dual-specific protein phosphatases while the number of dual-specific protein kinases is 395 [2]. Thus dual-specific phosphatases are important regulators in maintaining homeostasis of cell growth, proliferation and cell death. Phosphatase and TENsin homologue deleted on chromosome 10 (PTEN) is a dual-specific phosphatase, which has both lipid and protein substrates [3, 4]. PTEN/MMAC (Mutated in Multiple Advanced Cancers-1) was identified as a tumour suppressor gene from human chromosome 10q23.3 by positional cloning, homozygous deletions, and mutational analysis [5]. PTEN contains an N-terminal catalytic phosphatase domain, a C2-domain and a C-terminal tail containing two

PEST-motifs (proline, glutamate, serine, and threonine rich motif) and a PSD95, Dlg1, ZO-1 (PDZ)-binding domain [6–8]. It is the second most mutated gene after *TP53* in wide variety of human cancers [9].

The primary function of PTEN was understood because of its phosphatase activity to inhibit Phosphoinositide 3-kinase (PI3K)/protein kinase B (PKB/AKT) signalling cascade [9, 10]. PTEN is also a potential inducer of apoptosis in cancer cells and is regulated by AKT/ROS/p53/p21 signalling pathway [11]. The p73/PTEN protein complex acts as a co-activator of apoptosis [12]. Transmembrane Phosphatase with TEnsin homology (TPTE) and TPTE and PTEN homologous Inositol lipid phosphatase (TPIP) belong to the PTEN family of phosphatases and are expressed from human chromosome 13 and 21, respectively. Both TPTE and TPIP have multiple splice-variants, i.e., TPTEα, β, γ, δ and TPIPα, β, and γ mRNAs reported so far. TPIPα is reported to be a lipid phosphatase like PTEN [13, 14]. Recent advances in understanding functions of PTEN focus on much wider and essential roles, e.g., in development, maintenance of hematopoietic stem cells, cell growth regulation, apoptosis, cell migration, cell proliferation and chromosomal integrity [10]. These regulations need wild type PTEN or its C2-domain and C-terminal tail and operate through post-translational modification and direct protein–protein interaction with various cellular targets [10, 15–19]. Crystal structure, deletion and mutation studies of PTEN revealed that the C2-domain associates strongly with the N-terminal phosphatase domain to maintain the catalytic site and even small deletion of C2-domain removes detectable phosphatase activity [9, 16, 20]. The importance of C2-domain has also been studied with respect to cell migration, chromosomal stability, interaction with Thioredoxin-1 (Thx-1), Serine/Threonine Kinase 11 (STK11/LKB1), p53, transactivation of p53 and autoregulation of its own expression [15, 18, 21–24]. However, the role of isolated C2-domain in regulation of cell proliferation has not been reported. We studied the effect of a novel PTEN-like human TPIP cDNA (TPIP-C2) encoding a C2-domain in cell proliferation regulation and apoptosis. Overexpression of the 193 amino acid C2 domain of TPIP-C2 cDNA in human embryonic kidney (HEK-293) cells caused cell cycle arrest, inhibition of cell proliferation and induction of apoptosis, far more than overexpression of the full length human PTEN cDNA.

Materials and methods

Human TPIP-C2 cDNA

The TPIP-C2 cDNA (Genbank accession no. FJ969729) was isolated as a 1.019 kb cDNA [25] from a human testis cDNA library by screening with a novel 227 bp rat genomic simple repeat DNA probe (Genbank accession no. ×97459) in a previous study to isolate and identify mammalian candidate cDNAs containing simple repeat sequences [26].

Database searches and in silico analysis

The TPIP-C2 cDNA was sequenced and in silico analysis of the nucleotide sequence was performed. Prediction of domains, motifs were carried out by ELM (http://elm.eu.org/) and SMART (http://smart.embl-heidelberg.de/). Intrinsic protein disorder and globularity predictions were carried out by GlobPlot2.3 (http://globplot.embl.de/). Kyte-Doolittle hydrophobicity plot and CLUSTALW analyses were carried out by BioEdit (http://www.mbio.ncsu.edu/BioEdit/bioedit.html). Homology modelling of TPIP-C2 cDNA-predicted protein was performed by EasyPred (http://www.cbs.dtu.dk/biotools/EasyPred/) by using the PTEN crystal structure (PDB ID:1D5R) as a template. The model was refined by using MODLOOP (http://modbase.compbio.ucsf.edu/modloop///modloop.html) and the quality was checked by using SAVES (http://nihserver.mbi.ucla.edu/SAVES/). The model of TPIP-C2 was superimposed with the human PTEN structure (by Superpose (http://wishart.biology.ualberta.ca/SuperPose/) [27].

Cell line, plasmids, oligonucleotides, antibodies, and reagents

Molecular biology and tissue culture grade reagents were purchased from Sigma-Aldrich, USA; Metafectene™Pro (Biontex, Germany), synthetic oligonucleotides (Microsynth, Switzerland), MMLV-RT and RNasin (Promega, USA), PTEN425A monoclonal antibody (a kind gift), monoclonal anti-β-actin mouse antibody (A5316), anti-HA-antibody (H9658), monoclonal anti-PARP antibody (P248), anti-caspase 3 (active) antibody (C8487), MTT (M2128), propidium iodide (P4170), antimouse HRP-conjugated secondary antibody and antirabbit HRP-conjugated goat secondary antibody were all purchased from Sigma-Aldrich. Mammalian expression plasmids: pCMV-PTEN (a kind gift) [28], pcDNA-TPIP-C2 (the full length TPIP-C2 cDNA was cloned into Eco RI site of pcDNA 3.1 vector) [25], pCMV-βgal (the *E. coli* β-galactosidase protein coding sequence was cloned downstream of CMV promoter/enhancer), pEGFP-N2 plasmid (Clontech, USA, a kind gift), human embryonic kidney (HEK-293) cells (ATCC, U S A) were used for the study. TPIP-ORF refers to the 193 aa coding region of TPIP-C2 [25]. To check the expression of transfected TPIP-C2 protein, a nine aa HA-tag was introduced in the full length pcDNA-TPIP-C2 plasmid just before the stop codon in the TPIP-C2 ORF by circular PCR using *Pfu* Turbo DNA polymerase (Stratagene) and Dpn I digestion to generate pcDNA-TPIP-C2-HA tagged plasmid.

Transfection of human embryonic kidney (HEK-293) cells

HEK-293 cells were grown up to 75% confluency in T-25 flasks containing DMEM, 10% FBS with antibiotics and antimycotic in a humidified 37°C and 5% CO_2 incubator. The cells were seeded at 0.1×10^6/ml density in 2 ml medium in six-well plates. The medium was changed after 15 h and transfection was carried out in duplicates within 18 h after seeding with pcDNA-TPIP-C2, pcDNA-TPIP-C2-HA or pCMV-PTEN plasmid DNA at different amounts (0, 1.0, 2.0 μg) in a total amount of 2 μg DNA per well compensated with vector DNA (pcDNA 3.1) for 6 h by using Metafectene-pro reagent as per the manufacturer's instructions. The pEGFP-N2 plasmid was transfected to assess the transfection efficiency by GFP-fluorescence. The transfection medium was replaced by fresh medium after 6 h and the cells were allowed to grow. After 24 h post-transfection, the cells were visualized and photographed by a phase-contrast microscope. The floating and attached cells were harvested separately and counted by a Haemocytometer. For RNA isolation and RT-PCR, the floating and attached cells were pooled from duplicate wells and processed accordingly.

RNA isolation and reverse transcription-PCR (RT-PCR)

RNA was isolated by TRI-reagent (Sigma), first strand cDNA was synthesized from 1.0 μg of RNA, 0.5 μg oligo$(dT)_{15}$, 0.5 mM dNTPs, 20 U RNasin and 100 U M-MLV-RT in RT-reaction buffer (Promega) in 25 μl. First strand cDNAs (1.0 μl for GAPDH and 2.5 μl for TPIP-ORF and TPIP-C2) were used as templates for PCR in 25 μl. The following primers were used for PCR/RT-PCR.

GAPDH :5′-ACCACAGTCCATGCCATCAC-3′ (forward)
5′-TCCACCACCCTGTTGCTGTA-3′ (reverse)

TPIP-ORF : 5′-AAGAATAAGCTTATGGTTTGTGCCCT CCTTATTG-3′(forward)
5′-TCATTGAAGCTTCATTTCTCGCCAAA AAGTATCTCCA-3′(reverse)

TPIP-C2 : 5′-ATACCATGTATGTTCTTGAACT-3′ (forward)
5′-GGATTGGAGAGCGGGGATT-3′(reverse)

The reaction contained 1× PCR buffer, 0.2 mM dNTPs, 2.0 mM $MgCl_2$, 12.5 pmol of each primer, 1.0–2.5 μl first strand cDNA template and 1.0 U Taq DNA polymerase (Biotools). The PCR cycle parameters were as follows: denaturation at 94°C for 4 min, 35 cycles of 94°C for 45 s; 68°C (TPIP-ORF) or 51°C (TPIP-C2), 60°C (GAPDH) for 45 s–1 min; 72°C for 1 min and final extension of 10 min at 72°C. The amplicon sizes were TPIP-ORF (603 bp) for the C2-ORF of human TPIPα, γ, TPTEα, β, γ; TPIP-C2-specific (733 bp) and GAPDH (452 bp). One-tenth (2.5 μl) of GAPDH and one-fifth (5 μl) of TPIP-C2 PCR products were analyzed by 1.5% agarose-TBE gels, photographed by an AlphaImager 3400 gel documentation system and the signal intensity was measured by densitometry (Integrated Density Value) by the AlphaImager software. The data were represented as Mean ± SEM from three independent experiments.

Western blot analysis

The cells were harvested either at 24 h or at 36 h post-transfection, washed with cold PBS (phosphate buffered saline) and lysed in cold lysis buffer (20 mM Tris–HCl, pH 8.0, 250 mM NaCl, 1 mM DTT, 2 mM EDTA, 1% Triton X-100, 10 μg/ml leupeptin, 10 μg/ml aprotinin, 0.5 mg/ml benzamidine, 1.0 mM PMSF and 2 mM sodium orthovanadate). After 30 min incubation on ice, the lysates were cleared by centrifugation at $12{,}000 \times g$ for 10 min at 4°C. Protein concentration was estimated by Bradford assay. Approximately, 30–60 μg proteins were resolved by 10% SDS-PAGE and transferred to nitrocellulose membrane (Bio-Rad). Western blot was carried out for TPIP-C2-HA, PTEN, PARP, active caspase 3, and β-actin using the respective antibodies, and the blots were developed by Super Signal West Pico Chemiluminescence reagent (Pierce). The signal intensity was estimated by densitometry.

In situ β-galactosidase staining and apoptosis

HEK-293 cells (0.1×10^6/ml) were co-transfected with 0.5 μg of β-galactosidase expression plasmid along with 2.0 μg of PTEN or TPIP-C2 expression plasmid in 2 ml medium per well in six well plates for 6 h. After 24 h post-transfection, the medium was removed, the cells were washed with PBS, fixed in 1 ml of 0.05% glutaraldehyde for 15 min, washed with three changes of PBS for 20 min and stained with X-Gal solution [0.2% X-Gal, 2 mM $MgCl_2$, 5 mM $K_4Fe(CN)_6.3H_2O$, 5 mM $K_3Fe(CN)_6$) in PBS] in a humidified 37°C incubator for 6 h to overnight and then stored in 50% glycerol at 4°C. The cells were visualized and photographed in a phase-contrast microscope at 400× magnification. For quantitation, cells from 7 to 10 different fields were counted per experiment and 20 to 60 blue (transfected) cells per individual field were considered for assessment of morphology. Cytoplasmic shrinkage, nuclear condensation and membrane-blebbing

were considered as the morphological parameters for apoptosis. In parallel experiments, the cells were transfected with TPIP-C2, PTEN expression plasmids and the attached and floating cells from each well were separately collected and counted. The data are presented as Mean ± SEM from three independent experiments.

DNA fragmentation assay

DNA fragmentation was assayed as an end-point of apoptosis by extracting genomic DNA from the HEK-293 cells transfected with the pcDNA-TPIP-C2, pCMV-PTEN and vector plasmids at 36 h post-transfection as described earlier [29]. Briefly, the culture medium was removed and centrifuged at 3,000×*g* for 5 min to collect the floating cells and pooled with the adherent cells. The cells were lysed in 0.5 ml lysis buffer (10 mM Tris–HCl, pH 7.4, 5 mM EDTA, 0.2% Triton X-100) and incubated on ice for 30 min. The supernatant was collected and divided into 250 µl aliquots. To each aliquot, 50 µl ice-cold 5 M NaCl was added and the DNA was precipitated by adding 150 µl of 3 M Na-acetate, pH 5.2 and 0.6 ml cold ethanol. The DNA was collected by centrifugation, dissolved in 200 µl dissolving buffer (10 mM Tris–HCl, 5 mM EDTA) and treated with 2 µl (10 mg/ml) DNase-free RNase followed by 0.5 mg/ml Proteinase K, each at 55°C for 1 h. The DNA was precipitated, the DNA-pellet was recovered by centrifugation, redissolved in the buffer and electrophoretically separated on a 2% agarose gel containing 1 µg/ml ethidium bromide and visualized under ultraviolet transilluminator and photographed.

Cell proliferation measurement by cell viability (MTT) assay

Seventy thousand cells were plated per well in a 24-well plate and transfected in triplicates with 0.25, 0.5 µg of PTEN and TPIP-C2-HA plasmid for 6 h by using Metafectene-pro. After 36 h post-transfection, 100 µl MTT (5 mg/ml) was added to each well and incubated at 37°C. After 2 h, MTT crystals were solubilized by adding 500 µl of MTT solvent (5 mM HCl, 0.1% Nonidet P-40 in isopropanol) and incubated for another 1 h at 37°C. The absorbance was measured at 590 nm by a spectrophotometer. The data was represented as mean ± SEM from three independent transfections and each experiment was repeated twice.

Cell cycle analysis

HEK-293 cells in a six-well plate were transfected with TPIP-C2-HA plasmid as described above and harvested 36 h post-transfection. Cells were trypsinized, washed twice with ice-cold PBS, fixed in 70% ethanol in ice-cold PBS for 2 h at 4°C. The cells were incubated with 0.1 mg/ml RNase A at 37°C for 1 h, stained with 50 µg/ml propidium iodide for 15–20 min on ice, and then measured by flow cytometry by using FACSCalibur (Becton–Dickinson) and CellQuest software for data acquisition and analysis. A minimum of 20,000 events were recorded for each sample.

Results

Predicted structure, regulation and modifications of TPIP-C2 protein

The human TPIP-C2 (Genbank accession number FJ969729) is a variant mRNA produced from the TPIP locus on human chromosome 13. Multiple sequence alignment of the 193 aa ORF of TPIP-C2 with ten other members of the human and murine PTEN/TPIP/TPTE family by Clustal W analysis is shown in Fig. 1. It shows that TPIP-C2 has significant identity with TPIPα (253–445 aa), TPIPβ (199–326 aa), TPIPγ (330–522 aa) and similarity with TPTEα (348–540 aa), TPTEβ (330–522 aa), TPTEγ (310–502 aa), TPTEδ (210–402 aa), mouse TpteA (468–664 aa), mouse TpteB (449–645 aa) and human PTEN (134–350 aa) in the C2-domain. There is a 34 aa unique polypeptide in human PTEN starting at 284 aa immediately following the CBRIII motif (loop region) and another 24 aa unique polypeptide ending with 373, which represent signature sequences of the PTEN. TPIP-C2 lacks the signature lipid phosphatase active site, suggesting that it is a new variant without a lipid-phosphatase activity. The 5′-UTR (1-339 nt.) is followed by the 193 aa ORF containing a translational start site (ATG, Methionine), a partial phosphatase domain and a C2-domain. In order to probe into its property, the C2 domains of PTEN, TPIP-C2 and TPTE were analyzed for hydrophobicity (Fig. 2). The 5′-UTR of TPIP-C2 cDNA contains an Alu-Sx (145–241 nt.) SINE (short interspersed nuclear element) and a L3CR1 (268–328 nt) LINE (long interspersed nuclear element) repeat sequences (Fig. 3a), due to which the TPIP-C2 cDNA was isolated by the simple repeat DNA probe from the human testis cDNA library. TPIP-C2 shows characteristic hydrophobicity, which is different from its homologue, TPTE (348–540 aa of TPTEα) and PTEN (134–350 aa) (Fig. 2a). It differs in the central region (~70–140 aa of TPIP-C2), which is more hydrophobic but the N-terminal and the C-terminal regions show similar patterns with TPTE and PTEN. Distinct alternate hydrophobic and hydrophilic regions are clearly observed as peaks in the C2-domian of PTEN but this feature is less pronounced in TPIP-C2 and TPTE C2-domains. TPIP-C2 is predicted to be a globular protein like

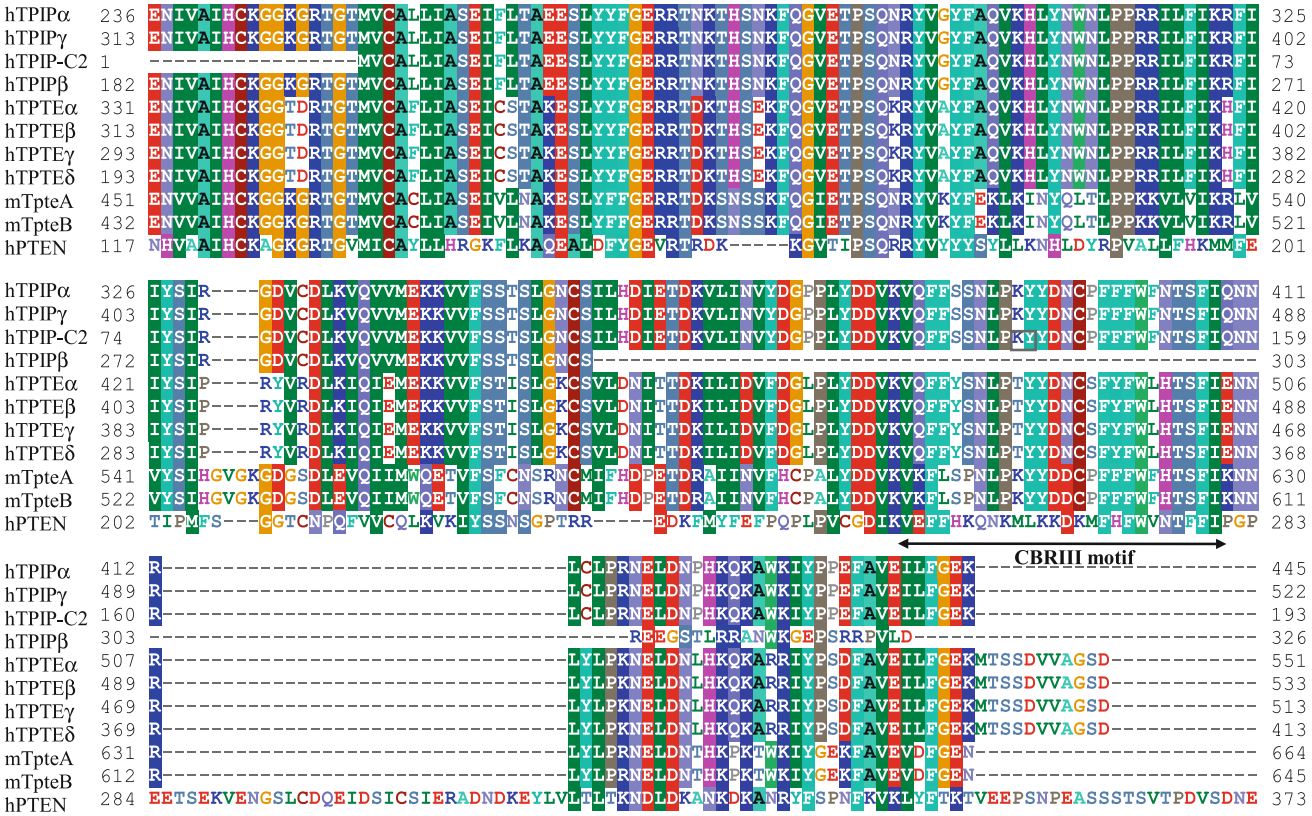

Fig. 1 TPIP-C2 belongs to the PTEN/TPIP/TPTE family of dual specificity phosphatases. Multiple alignment of amino acid sequences is shown for human TPIPα, *β*, *γ*, TPTEα, *β*, *γ*, *δ*, PTEN, mouse TpteA, TpteB and human TPIP-C2. The 1–193 aa of TPIP-C2 shows similarity with human TPIPα (253–445 aa), *β* (199–326 aa), *γ* (330–522 aa), TPTEα (348–540 aa), *β* (330–522 aa), *γ* (310–502 aa), *δ* (210–402 aa), mouse TpteA (468–664 aa), TpteB (449–645 aa) and human PTEN (134–350 aa). The polybasic CBRIII motif is marked. H *Homo sapiens*, m *Mus musculus*

C2-domains of TPTE and PTEN. C2-domain of TPTE does not show any disorder sequence but C2-domains of PTEN and TPIP-C2 have three short disorder sequences (Fig. 2b) at different positions. The disorder sequences of TPIP-C2 and PTEN-C2 were aligned and found to differ in terms of their position and sequence (Fig. 2b, right panel). These short disorder sequences are expected to fall in the loop region and are available, projecting outwardly from the globular region and may act as sites for protein–protein interactions. These disorder sequences may provide more functional flexibility to a protein [30]. Interestingly, the 193 aa ORF (340–921 nt.) of TPIP-C2 is predicted to have several motifs, domains and post-translational modification sites (Fig. 3a). It has a partial phosphatase domain (1–56 aa) and a C2-domain (56-193 aa), the latter is identical to that of TPIPα, *γ* and homologous to TPTEα, *β*, *γ*, *δ* and PTEN of humans. A 18 aa signal peptide at the N-terminus; four protein kinase C (PKC) phosphorylation sites at amino acid positions 27–29 [TNK], 32–34 [SNK], 76–78 [SIR], 112–114 [TDK]; one Casein Kinase II (CKII) phosphorylation site at position 14–17 [TAEE]; three *N*-glycosylation sites (ASN) at positions 28–31 [NKTH], 103–106 [NCSI] and 152–155 [NTSF]; a 'RGD' cell attachment sequence at 78–80 were also identified (Fig. 3a). A homology model for the 192 aa (the last aa lysine was not included in the structure) of TPIP-C2 ORF was built (Fig. 3b, left panel) using the PTEN structure (PDB ID: 1DR5) as the template.

The Ramachandran plot (Supplementary Fig. 1) for PTEN and the plot statistics show that PTEN does not have any residue in the disallowed region but has 3.6% residues (ten residues) in generously allowed regions, but in case of TPIP-C2, it has 0.6% residues (Glu 91) in generously allowed regions and 0.6% (Asp 127) in disallowed region. Considering Ramachandran plot and other structural parameters, the TPIP-C2 model quality is satisfactory. The TPIP-C2 model was superimposed with the PTEN structure and it showed a very strong overlap and similarities with PTEN-C2 domain implying that TPIP-C2 is structurally very close to the PTEN-C2 domain (Fig. 3b, right panel). Thus in silico analysis of the TPIP-C2 cDNA-predicted protein revealed that it is a globular protein like the PTEN, but it has a partial N-terminal phosphatase domain and functional modification sites in the loops projecting out

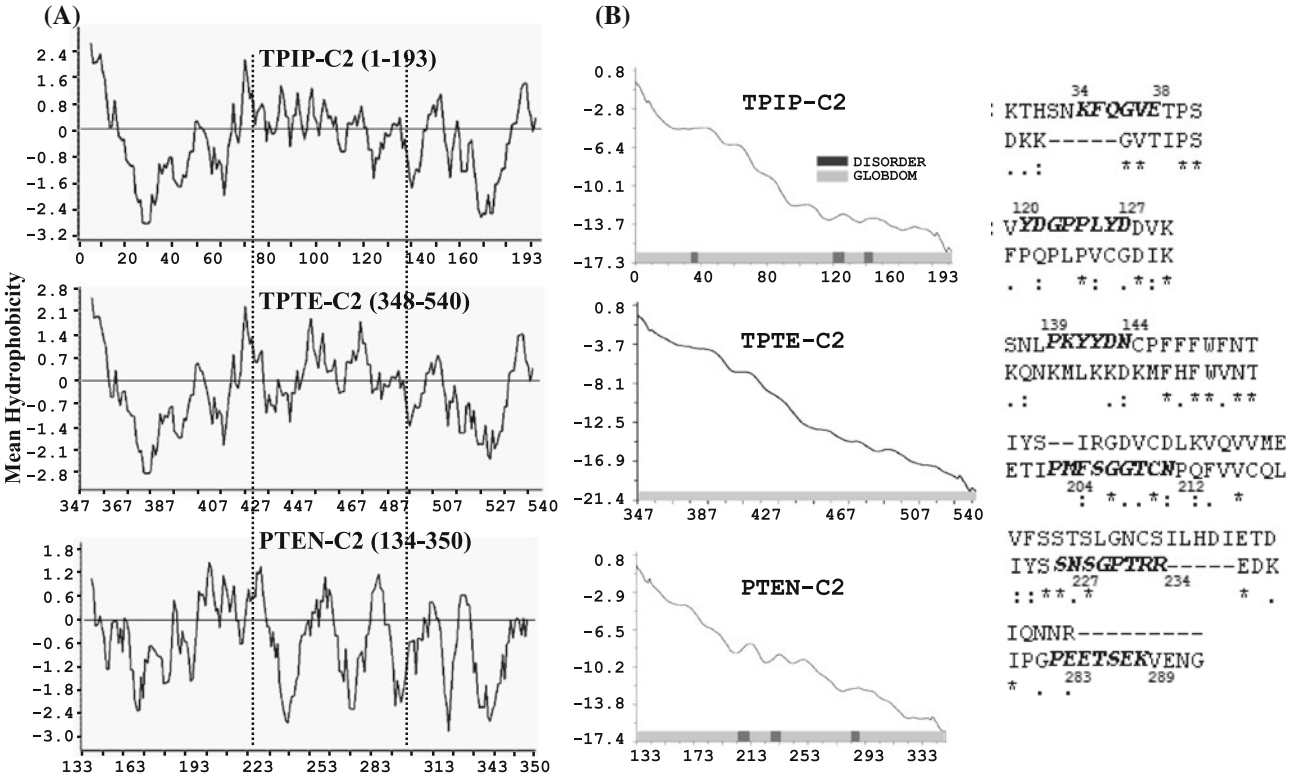

Fig. 2 Properties of the TPIP-C2 cDNA-predicted protein. **a** Comparison of hydrophobicity profiles of the C-2 domains of TPIP-C2 (1–193 aa), PTEN (134–349 aa) and TPTE (348–540 aa of TPTEα). The central region of TPIP-C2 is more hydrophobic as compared to those of PTEN and TPTE. **b** Comparison of intrinsic disorder sequences and globular domain of TPIP-C2, PTEN and TPTE by GLOBPLOT2 (*left panel*). Alignment of the disorder regions (*bold in the top sequence*) of TPIP-C2 (*top three*) and PTEN (*bottom three*) are shown (*right panel*). *Asterisk* denotes identical, conserved and semi-conserved substitutions, respectively

from the globular structure. We hypothesized that because of the absence of the C-terminal tail, which is shown to act as an autoinhibitory domain in the PTEN [31], TPIP-C2 may be a more active C2-domain in cells in terms of its function. This was tested by overexpression of TPIP-C2 cDNA in the HEK-293 cells.

Overexpression of TPIP-C2 cDNA inhibits cell proliferation and causes apoptosis

Earlier work from our laboratory showed that ectopic expression of the full length TPIP-C2 cDNA from a pcDNA expression plasmid in the human cervical carcinoma (HeLa) cells caused suppression of cell growth/proliferation as judged by stable transfection and G418-resistant colony formation assay [25]. This was expected for a tumor suppressor homologous protein. We studied effect of overexpression of TPIP-C2 cDNA on cell cycle, cell proliferation and apoptosis in the HEK-293 cells. Similar expression of full length human PTEN cDNA, a well known tumor suppressor, was used for comparison. Expression of TPIP-C2 RNA was measured by RT-PCR and expression of PTEN was determined by western blot analysis. Since TPIP-C2 cDNA has extensive sequence homology with other members of the PTEN/TPIP/TPTE family, a specific RT-PCR assay was developed to distinguish TPIP-C2 RNA from other TPIP-isoforms. The TPIP-ORF-primers were used to amplify a 603 bp TPIP-ORF from TPIPα, γ, δ and -C2 transcripts and the TPIP-C2 primers were used to specifically amplify the 733 bp DNA only from the TPIP-C2 transcript but not from the related transcripts. Figure 4a shows that untransfected (C) and vector transfected (V) HEK-293 cells express basal levels of mRNAs for TPIP-isoforms as shown by the 603 bp DNA amplified by ORF-primers and TPIP-C2 as shown by the 733 bp DNA amplified by TPIP-C2 primers. Transfection of 1 and 2 μg of TPIP-C2 cDNA resulted in overexpression of TPIP-C2 mRNA as shown by increased levels of the 733 bp (and also 603 bp) amplicon in comparison to cellular GAPDH mRNA levels showing no change in the 452 bp amplicon (Fig. 4a). This is the first report of endogenous TPIP-C2 mRNA expression in HEK-293 cells. These cells also express other TPIP-variants as suggested by the level of TPIP-ORF RNA expression detected by RT-PCR, which is much higher than the TPIP-C2 product (Fig. 4a). The western blot shows that PTEN

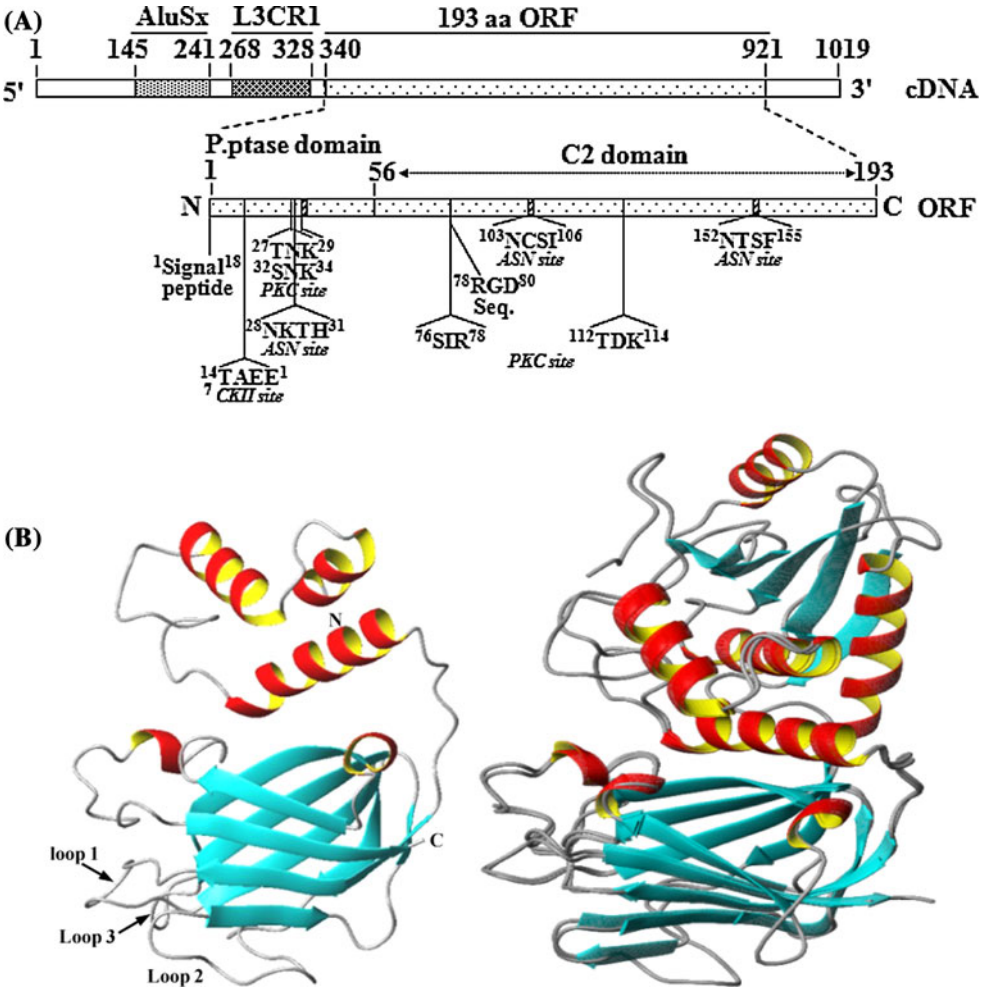

Fig. 3 Structural domains and post-translational modification sites in the TPIP-C2 cDNA-predicted protein. **a** Organization of TPIP-C2 cDNA showing the SINE, LINE in 5′-UTR, 193 aa ORF depicting a partial phosphatase domain, a C2-domain and the predicted post-translational modification sites. *PKC* protein kinase C phosphorylation site, *CK II* casein kinase II phosphorylation site, *ASN N*-glycosylation site, *RGD* Cell attachment sequence, *P-ptase domain* partial-phosphatase-domain. **b** Ribbon model of the TPIP-C2 protein was built by homology modelling using PTEN (PDB Id:1D5R) as template (*left*). The TPIP-C2 structure was superimposed with the structure of PTEN (*right*)

protein is very weekly expressed in HEK-293 cells and the amount of PTEN protein greatly increased with increasing amount of PTEN cDNA transfected into the cells in comparison to the cellular β-actin protein (Fig. 4b). To detect the TPIP-C2 protein in the transfected cells, we inserted a HA-tag in the pcDNA-TPIP-C2 expression plasmid to make pcDNA-TPIP-C2-HA expression plasmid. Expression of HA-tagged TPIP-C2 protein is shown as a band of $\sim$30 kDa in transfected HEK-293 cells (Fig. 4c). The transfection efficiency was $\sim$80 to 90% as determined by transfection of 2 μg of pEGFP-N2 plasmid into the HEK-293 cells (Fig. 4d). To investigate the effect of over-expression of TPIP-C2 cDNA, the morphology of the PTEN- and TPIP-C2 transfected cells were observed under a bright field microscope and the number of attached cells and floating cells were counted 24 h after transfection (Fig. 5). The TPIP-C2- and PTEN-transfected cells showed clearly altered morphology compared to the vector transfected cells (Fig. 5a) and the number of floating cells increased to a great extent in the TPIP-C2 transfected cells (1.45×10^5 for 2 μg of TPIP-C2 cDNA), which accounts for almost 50% of the total cells (Fig. 5a). In comparison to the untransfected cells (5.8×10^5) and vector transfected cells (5.79×10^5 for 2 μg of pcDNA), PTEN-transfected cells (4.03×10^5 for 2 μg PTEN cDNA) and cells transfected with TPIP-C2 (3.06×10^5 for 2 μg TPIP-C2 cDNA) showed significant decrease in the total number of cells and increase in the number of floating cells. Thus the total number of cells decreased almost 50% and again about 50% of the cells became floating due to overexpression of TPIP-C2 indicating inhibition of cell proliferation (Fig. 5b). We observed that the number of attached cells was higher in PTEN- than TPIP-C2-transfected cells but the number of floating cells was higher in TPIP-C2- than PTEN-transfected cells. This shows that PTEN can arrest cell growth and TPIP-C2 causes inhibition of attachment of cells to the plate and inhibition of cell proliferation. To further validate the growth inhibitory effect of TPIP-C2 on HEK-293 cells, cell proliferation was quantitated by a cell viability assay (MTT assay) in TPIP-C2 transfected HEK-293 cells at 36 h post-transfection. As shown in Fig. 5c, the cell proliferation inhibition increased from 15 to 28% in PTEN (from 0.25 to 0.5 μg DNA) transfected cells, while in case of TPIP-C2-HA transfected

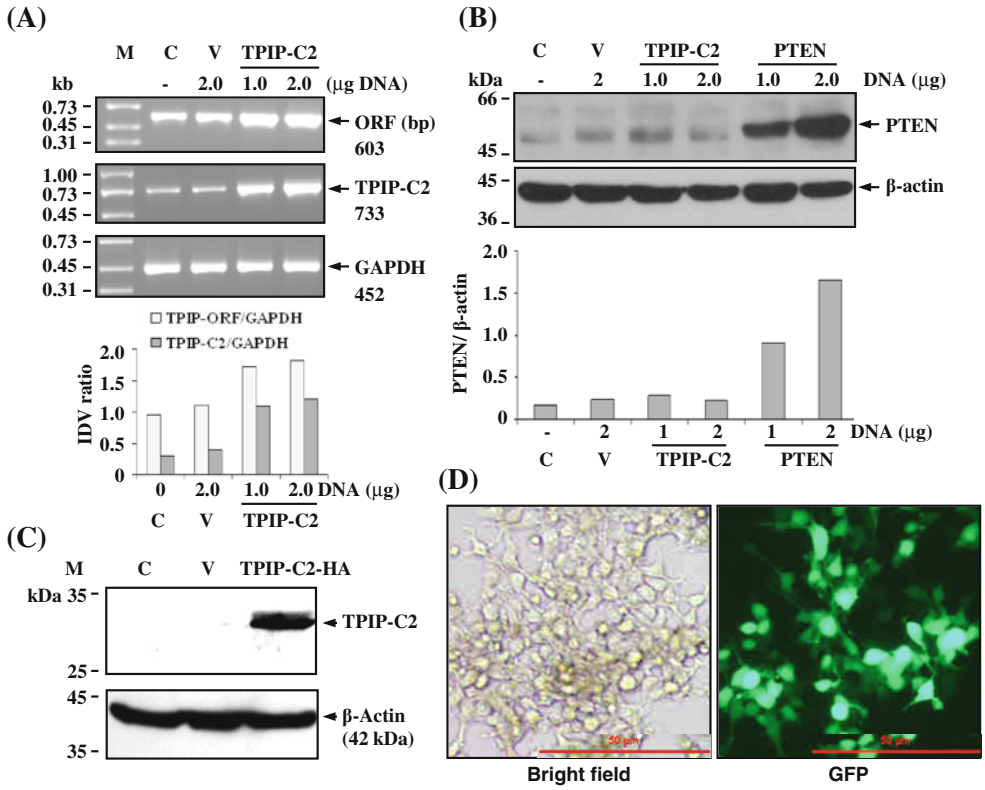

Fig. 4 Overexpression of TPIP-C2 cDNA in HEK-293 cells. **a** HEK-293 cells were transfected with mammalian expression plasmid containing the 193 aa ORF of TPIP-C2 cDNA (1 and 2 μg of pcDNA-TPIP-C2) or 2 μg of pcDNA vector DNA (V) and compared with control HEK-293 cells without any DNA transfection (**c**). Total amount of DNA transfected into cells was compensated by the vector DNA up to 2 μg DNA per well of six well plate. Expression of TPIP mRNA was measured by RT-PCR using ORF-primers (603 bp amplicon, *upper panel*), TPIP-C2-specific primers (733 bp amplicon, *middle panel*) and RT-PCR of cellular GAPDH mRNA (452 bp amplicon, *lower panel*) is shown as an internal reference. RT-PCR products were measured as integrated density value (IDV) by densitometry, normalized as IDV ratios of TPIP-ORF/GAPDH and TPIP-C2/GAPDH and presented as *bar diagram*. **b** HEK-293 cells were transfected with full length human PTEN cDNA (1 and 2 μg pcDNA-PTEN plasmid), pcDNA-TPIP-C2 plasmid (1 and 2 μg) and 2 μg of pcDNA vector (V). Expression of PTEN protein was measured in 30 μg of whole cell extract by western blot analysis using anti-PTEN antibody (*upper panel*). Expression of cellular *β*-actin protein (42 kDa) detected by western blot analysis using anti-*β*-actin antibody is shown as an internal reference (*lower panel*). Western blot signals were measured as integrated density value (IDV) by densitometry, normalized as IDV ratio of PTEN/*β*-actin and presented as *bar diagram*. The data in **a** and **b** represent average of two independent experiments. **c** Expression of HA-tagged TPIP-C2 protein in TPIP-C2-HA DNA (2 μg) transfected HEK-293 cells by western blot using anti-HA antibody. **d** HEK-293 cells were transfected with 2 μg CMV-enhanced GFP (pEGFP-N2) plasmid and transfection efficiency (~80–90%) was calculated by counting ~1,000 cells/well. *M* molecular size marker, *kb* kilo base pair, *C* control HEK-293 cells, *V* pcDNA3.1 vector transfection

cells the inhibition was 36% and 49% with increase in the amount of DNA transfected, from 0.25 μg to 0.5 μg (Fig. 5c). The vector transfected cells grew up to similar extents as the untransfected cells indicating there was no effect due to the transfection reagent or method used. The above results validate that TPIP-C2 is a more potent inhibitor of cell proliferation in comparison to PTEN. In order to study apoptosis, we then checked for the caspase 3 activation and PARP cleavage by TPIP-C2. Figure 5d shows that immunoblot analysis of cell extracts from the TPIP-C2 transfected cells clearly demonstrate activation of caspase 3, which plays a central role in the execution of apoptotic program. The 17 kDa fragment is activated in the PTEN and TPIP-C2-HA over-expressed cells but not in the control cells transfected with vector DNA. The amount of active caspase 3 in the TPIP-C2-HA overexpressed cells was much higher in comparison to the PTEN overexpressed cells. Caspase 3 is responsible for cleavage of poly (ADP-ribose) polymerase (PARP) as a cellular target. The intact 118 kDa PARP was cleaved into an 89 kDa fragment in the PTEN and TPIP-C2-HA overexpressing cells (Fig. 5d), this is another hallmark of the cells undergoing apoptosis [32]. Thus overexpression of TPIP-C2 in HEK-293 cells drastically inhibited cell proliferation and induced apoptosis. To observe morphology of the apoptotic cells, we cotransfected HEK-293 cells with one-fifth (0.5 μg) of CMV-*β*-galactosidase expression plasmid mixed with the TPIP-C2 expression plasmid (2.0 μg) and the attached cells

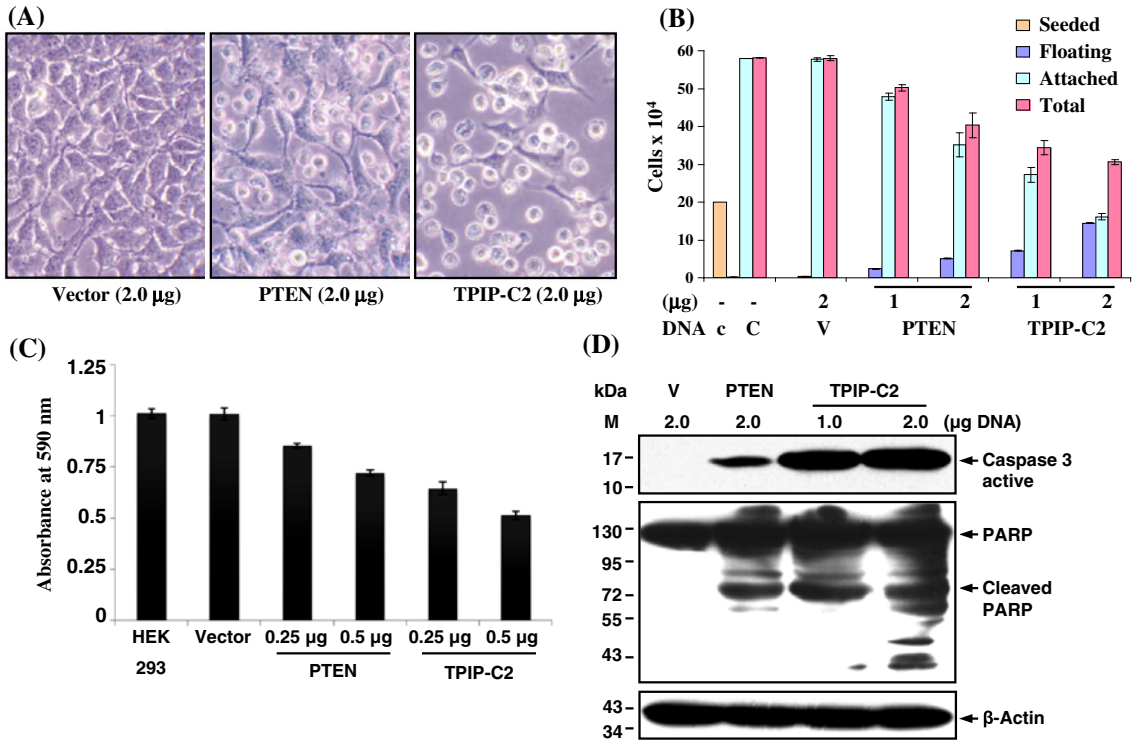

Fig. 5 Inhibition of cell proliferation and induction of apoptosis by TPIP-C2 in HEK-293 cells. **a** Morphology of HEK-293 cells after transfection with 2 µg of TPIP-C2 cDNA or PTEN cDNA showing attached and floating cells at 24 h post-transfection as visualized under bright field microscope. This is representative of four independent experiments. **b** The numbers of total, attached and floating cells are presented as *bar diagram*. The data represents mean ± SEM of three independent experiments. The number of floating cells increased and the number of attached cells decreased in the TPIP-C2 transfected cells in comparison to vector and PTEN-transfected cells. **c** HEK-293 cells were transfected with PTEN and TPIP-C2-HA DNA (0.25 and 0.5 µg DNA in a total of 0.5 µg of DNA per well in 24-well plate in triplicates). Viable cells were quantitated by using MTT assay 36 h post-transfection. *Data plotted* shows mean ± SEM of triplicate wells. **d** HEK-293 cells were transfected with pCMV-PTEN plasmid (2 µg), pcDNA-TPIP-C2-HA plasmid (1 and 2 µg) or pcDNA vector DNA (2 µg). Expression of active caspase-3 (cleaved caspase-3) and PARP was detected in cell extracts by western blot analysis using the specific antibodies. Expression of cellular *β*-actin protein is shown as an internal reference. *M* molecular size marker, *kb* kilo base pair, *c* initial number of cells seeded, *C* control HEK-293 cells (no transfection), *V* pcDNA3.1 vector transfection

were stained by X-Gal at 24 h post-transfection and *β*-galactosidase positive blue cells were scored (Fig. 6a). The TPIP-C2 and *β*-galactosidase co-transfected blue cells showed characteristic apoptotic morphology, e.g., distorted shape, extension of thin extracellular projections, cell shrinkage, chromatin condensation, irregular cell membrane and blebbing (Fig. 6a). By this assay, the percentage of apoptotic blue cells in the TPIP-C2 overexpressing and attached cells was 94–98%, whereas it was ∼12% in the PTEN overexpressing blue cells, and in the vector transfected control blue cells it was only ∼2% (Fig. 6a). Thus TPIP-C2 is ∼8× fold more potent than PTEN in causing apoptosis in HEK-293 cells. The high levels of floating cells, decrease in cell viability in the MTT assay and increase in the apoptotic, attached blue cells showed that the 193 aa C2-domain of TPIP-C2 cDNA strongly caused apoptosis in HEK-293 cells. Further, since DNA fragmentation is a reflection of chromatin-DNA degradation during apoptosis, we checked for DNA laddering in the TPIP-C2 transfected cells. DNA fragmentation (but not DNA laddering) was also clearly observed at 36 h post-transfection in the TPIP-C2-HA transfected cells. TPIP-C2 DNA at 1 µg showed almost similar extent of DNA fragmentation as in the 2 µg DNA transfected cells, PTEN (2 µg) did not show this effect (Fig. 6b). The DNA fragmentation very well correlates with the observation of apoptotic cell morphology by the blue cell assay described above. TPIP-C2-induced apoptosis was further confirmed by cell cycle analysis by measuring fluorescence from the cells stained for DNA with propidium iodide (Fig. 6c). With increase in TPIP-C2-HA DNA transfected, the percentage of cells in G1-phase decreased from 48% in vector DNA to 18% and 19% in 2 and 1 µg TPIP-C2 DNA and the percentage of apoptotic cells (AP) in sub-G1 region increased from 3.3% in the control (vector transfected) cells to 25% and 32% in the 1 and 2 µg TPIP-C2-HA DNA transfected cells, respectively, showing an increase in the population of hypodiploid, apoptotic cells due to decrease

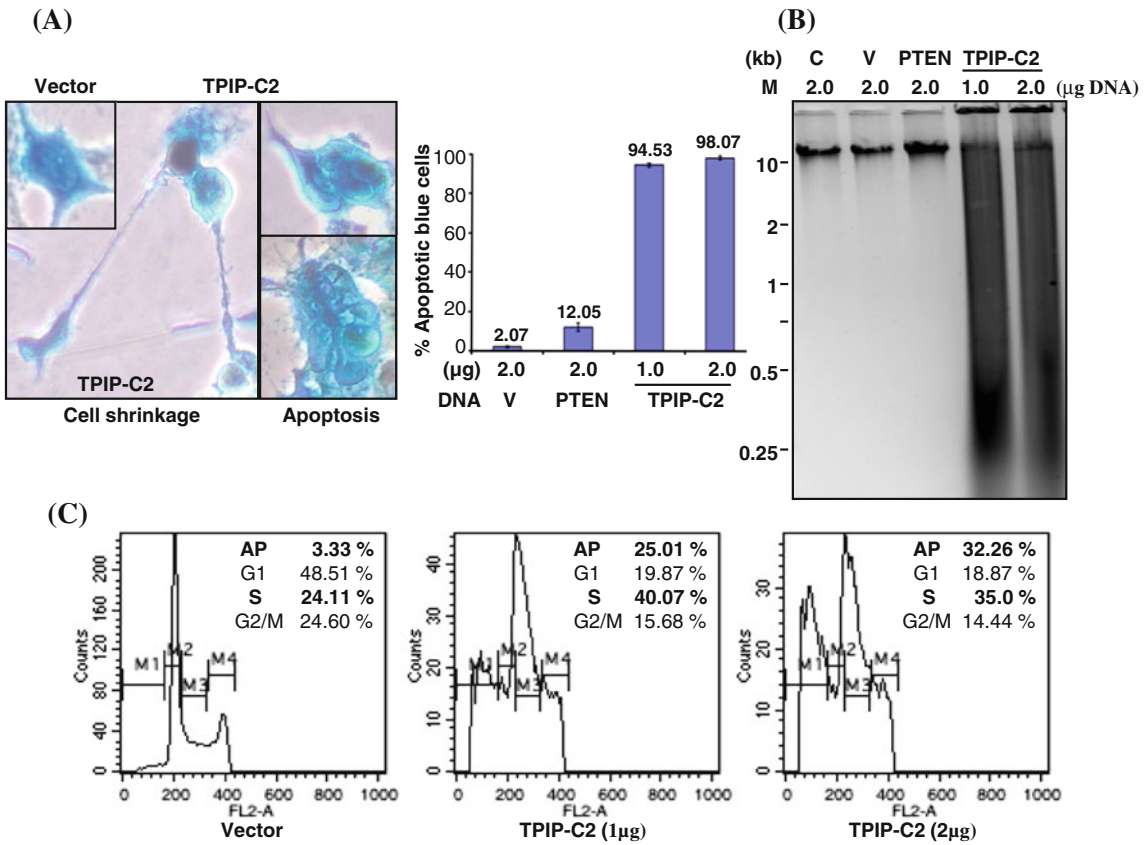

Fig. 6 Over-expression of TPIP-C2 in HEK-293 cells causes apoptosis. **a** Normal morphology of vector (2 μg) + *β*-galactosidase (0.5 μg) DNA transfected and X-Gal stained blue cells (×400) and apoptotic morphology of TPIP-C2 (2.0 μg) + *β*-galactosidase (0.5 μg) DNA transfected and X-Gal stained blue cells (×800) as visualized under bright field microscope. The cells were stained for *β*-galactosidase activity (*blue*) as mentioned in the methods. The percentage of apoptotic blue cells from three independent experiments is plotted with respect to the amount of DNA transfected as mean ± SEM. **b** DNA fragmentation assay of genomic DNA isolated from the untransfected (**c**), vector (V)-, PTEN- and TPIP-C2 DNA-transfected cells. **c** Flow cytometric analysis of HEK-293 cells transfected with TPIP-C2-HA plasmid. DNA was stained with propidium iodide and DNA content per cell was determined by flow cytometry 36 h post-transfection. Data are presented as percentage apoptotic (M1), G1 phase (M2), S-phase (M3) and G2/M phase (M4) cells. This is representative of two independent experiments. *AP* Apoptotic, *Vector* transfected with 2 μg pcDNA 3.1 plasmid, *M* molecular size marker, *kb* kilo base pair

in the DNA content per cell. TPIP-C2-HA expression also elicited accumulation of HEK-293 cells in the S-phase from 24 to 35% and 40% in the 2 and 1 μg TPIP-C2-HA DNA transfected cells, respectively. The vector transfected cells were not influenced. These results clearly demonstrate that TPIP-C2 is a potent activator of cell proliferation inhibition, cell cycle arrest and apoptosis in HEK-293 cells.

Discussion

TPIP-C2 is a novel human TPIP-isoform

During our earlier study, we identified the TPIP-C2 cDNA as one of the several cDNAs isolated from a human testis cDNA library by screening with a rat genomic simple repeat DNA (×97459) probe with an attempt to identify and characterize cDNAs with simple repeat sequences, which would represent cellular RNAs with repeat sequences [25]. The simple repeat DNA containing the $(GA/CT)_n$ mirror repeat showed homology with a variety of mammalian mRNAs due to presence of the repeat sequences in the mRNAs. These repeat sequences were present in the 5′-untranslated region (5′-UTR), 3′-UTR and exons of the mRNAs. It would therefore represent either repeated amino acids in the proteins or regulatory sequences in the mRNAs. The TPIP-C2 cDNA has a SINE (Alu-Sx) and a LINE (L3CR1) sequence in its 5′-UTR, which helped its isolation. Analysis of the nucleotide sequence of TPIP-C2 cDNA identified it as a novel splice-variant mRNA from the TPIP locus on human chromosome 13 and belonging to the PTEN/TPIP/TPTE family of dual specificity phosphatases [33]. The 193 aa ORF of TPIP-C2 cDNA contains a partial phosphatase domain and a C2-domain and

represents a novel TPIP-isoform protein. TPIP-C2 mRNA is expressed in the human testis and in the mouse tissues. When overexpressed in the HeLa cells, TPIP-C2 caused inhibition of cell proliferation and induction of apoptosis. We compared the C2-domain of TPIP-C2 with that of PTEN and analyzed its function in HEK-293 cells in the present study.

C2-domain of TPIP-C2 has distinct properties

Figure 1 shows the amino acid sequence comparison of TPIP-C2 with ten other members of the PTEN/TPIP/TPTE family. Significant identity of TPIP-C2 with TPIPα, TPIPβ, TPIPγ; similarity with TPTEα, TPTEβ, TPTEγ, TPTEδ; mouse TpteA, TpteB and human PTEN in the C2-domain established it as a member of the PTEN/TPIP/TPTE family of phosphatases encoding a C2-domain. Comparative analysis of the C2-domains of TPIP-C2, PTEN and TPTE showed that the C2-domain of TPIP-C2 has characteristic hydrophobicity property, three unique disorder sequences (Fig. 2) and posttranslational modification sites (Fig. 3a). The PTEN C2-domain lacks the canonical Ca^{2+} ligands, and is similar to C2-domains of Ca^{2+}-independent PKC isotypes [34]. PTEN C2-domain differs from these C2-domains in that it lacks all but one (Asp-268) of the Ca^{2+} ligands and is thus unlikely to bind Ca^{2+} [7]. The C2-domain of TPIP-C2 also has Asp-145 at this position and is probably a Ca^{2+}-independent C2-domain similar to that of PTEN (Fig. 1). PTEN contains two solvent-exposed hydrophobic residues, Met-264 and Leu-265 at the CBRIII loop. This is a position where about half of the known C2-domains contain at least one hydrophobic residue, proposed to be crucial for insertion into the lipid bilayer of membranes [7]. TPIP-C2 has two hydrophobic residues at these positions, Lys-140 and Tyrosine-141, implying a possible membrane insertion role (Fig. 1). TPIP-C2 has a partial phosphatase domain and a C2-domain (Fig. 3a). Classically, C2-domains have been shown to have a stable β-sandwich forming a scaffold. This scaffold allows the emergence of variable loops at the top and bottom of the domain. These β-scaffolds help in autonomous folding and binding to phospholipids in a Ca^{2+}-dependent manner as shown for C2A-domain of synaptotagmin I [34]. Recently, the crystal structure of a Ca^{2+}-independent lactadherin C2-domain was determined, which also has a β-barrel core and several hydrophobic amino acids on the membrane-interactive surface. It also showed that the isolated C2-domain retains substantial membrane-binding property and the hydrophobic residues and Glycine residues are involved in membrane binding [35]. The presence of solvent-exposed hydrophobic amino acids is proposed to interact with lipid moieties of the membrane bilayer. Likewise, TPIP-C2 may be a globular protein (Fig. 2b), with a central distinct stretch of hydrophobic amino acids (Fig. 2a). It has the β-barrel core similar to C2-domain of PTEN and other C2-domain proteins. C2-domain of TPIP-C2 also has three loops (Fig. 3b, left panel), which are present in other Ca^{2+}-dependent and Ca^{2+}-independent C2-domain proteins. The TPIP-C2 structure superimposed very well over the PTEN structure in the partial phosphatase domain and C2-domain (Fig. 3b, right panel). TPIP-C2 has a flexible Asp-127, as part of a distorted β-turn, which falls within the disallowed region of the Ramachandran plot (Supplementary Fig. 1). TPIP-C2 has a N-terminal signal peptide, 'RGD' cell attachment motif (Fig. 3a) and a polybasic CBRIII motif (Fig. 1), which is known to play role in membrane interaction and orientation. Interestingly, the predicted post-translational modification sites of TPIP-C2 (Fig. 3a) map to the loop regions in its predicted structure (Fig. 3b). Taken together, it is likely that TPIP-C2 may encode a Ca^{2+}-independent C2-domain protein similar to that of PTEN (Fig. 3b) and may be membrane localized. PTEN is a well known tumour suppressor, mutated/deleted in a wide variety of human cancers. In addition to genetic mutations, somatic, germline and promoter mutations of PTEN are responsible for a wide variety of disorders like Cowden Disease, Bannayan-Riley-Ruvalcaba syndrome (BRSS), Glioblastoma, melanomas, endometrial cancer and many other cancers [9, 36]. Such mutations in PTEN may cause inactivation, conformational change and loss of interaction with other proteins. The primary cellular target of PTEN is the PI3-kinase/Akt pathway, which is negatively regulated by PTEN's lipid phosphatase activity and in turn it controls a wide variety of cellular events like cell survival, growth, proliferation, migration, differentiation, etc. [9, 10]. The C2-domain of PTEN associates with the N-terminal phosphatase domain to make the catalytic site and deletions in the C2-domain inhibits the phosphatase activity [16]. The C2-domain loop mutants (PTEN-P204S and PTEN-G251C), when expressed at low levels, showed complete loss of the phosphatase activity [7, 16]. Thus C2-domain of PTEN is crucial for its function. C2-domains comprise of approximately 130 aa residues and was first identified in protein kinase C. More than 70 C2-domain protein crystal structures are now available in the database (http://www.ncbi.nlm.nih.gov/sites/entrez) and they are known to perform multiple biological functions. Expression of C2-domain of PTEN in PTEN-null cells caused potent inhibition of cell migration [15] and it also inhibited directional cell migration in developing chick embryonic mesoderm [21]. Therefore, uncharacterized C2-domain proteins in the EST-database may provide important biological information. Other members of PTEN family may also perform related functions.

Overexpression of TPIP-C2 causes inhibition of cell proliferation and apoptosis

We hypothesized that expression of isolated C2-domain in cells may inhibit cellular functions. TPIP-C2 cDNA and human PTEN cDNA were overexpressed in HEK-293 cells (Fig. 4) and their effects on cell proliferation and apoptosis were measured (Fig. 5). TPIP-C2 mRNA is endogenously expressed in HEK-293 cells and its expression increased in a dose-dependent manner with increasing amount of TPIP-C2 cDNA transfected into the cells (Fig. 4a). TPIP-C2 protein expression was detected as a 30 kDa protein in the transfected HEK-293 cells (Fig. 4c). PTEN was also overexpressed in HEK-293 cells for comparison. There was no effect of over-expression of TPIP-C2 on expression of endogenous PTEN. Expression of TPIP-C2 mRNA caused inhibition of cell proliferation (Fig. 5a–c). With increased expression of TPIP-C2 mRNA, the number of floating cells greatly increased (Fig. 5a, b) and similar suppressive effect of TPIP-C2 was also detected by a quantitative cell viability/proliferation assay (Fig. 5c) suggesting that this was the effect of over-expression of C2-domain of TPIP-C2. Other hallmarks of apoptosis are activation of effector caspase 3, which then cleaves PARP. We observed expression of active caspase 3 and cleaved PARP protein as a result of overexpression of C2-domain of TPIP-C2 (Fig. 5d). Moreover, TPIP-C2+ β-galactosidase cotransfected and X-Gal stained blue cells showed several features of apoptotic cells, e.g., distorted cellular morphology, extension of thin extracellular projections, cell shrinkage, chromatin condensation, irregular cell membrane, blebbing (Fig. 6a) as well as the floating cells. Some TPIP-C2 transfected cells also showed elongated cell morphology, which was observed more in number in case of PTEN (Fig. 5a). This may reflect effect of overexpression of PTEN and TPIP-C2 in directing differentiation of some HEK-293 cells. The chromatin-DNA of TPIP-C2 transfected cells was degraded, it showed DNA fragmentation at 36 h post-transfection (Fig. 6b) and the per centage of apoptotic cells increased with the increase in the amount of TPIP-C2 DNA transfected, as detected by cell cycle analysis (Fig. 6c). There was also dramatic increase in the number of cells arrested in the S-phase of the cell cycle. There are recent reports suggesting that the S-phase arrest and apoptosis of cells are regulated by the checkpoint kinases [37]. This may be due to blockage of the S-G2 transition at specific check point. To identify the regulatory proteins involved in this effect, further investigation is needed. TPIP-C2 is more potent than PTEN in causing cell proliferation inhibition and apoptosis. This may be due to the C2-domain of TPIP-C2, which may form a cellular growth inhibitory complex by protein–protein interaction, where TPIP-C2 can act like a dominant negative mutant. Apoptosis of HEK-293 cells caused by TPIP-C2 was caspase 3-dependent and it also activated cleavage of PARP and induced DNA fragmentation indicating the complete pathway of apoptosis being activated in the cells. Recently, PTEN/AKT pathway has been shown to be involved in histone deacetylase inhibitor-induced cell growth inhibition and apoptosis of oral squamous cell carcinoma cells [38]. Other studies have highlighted importance of C2-domain in membrane binding and membrane localization in Ca^{+2}-dependent and Ca^{+2}-independent manner. For example, the C2-domain of Smurf1 ubiquitin ligase plays a key role in its localization to plasma membrane, promotes cell migration and ligase activity towards Rho A in a Ca^{+2}-independent manner [39]; C2-domain of PTEN has been demonstrated to inhibit cell migration, independent of its phosphatase activity [15]. Recently, C2 domain of PTEN has been shown to be responsible for inhibition of U6 snRNA transcription [40] and membrane binding of the cell death causing protein, perforin [41]. All these studies suggest crucial role of C2-domain of PTEN for its tumor suppressor activity by regulating cell migration, localization and other activities. Our results taken together suggest that TPIP-C2 is a novel TPIP-isoform generated from the TPIP locus on human chromosome 13 and it may be expressed as a membrane localized C2-domain protein, which inhibits cell proliferation and promotes apoptosis in human embryonic kidney (HEK-293) cells. TPIP-C2 may be regulated by phosphorylation and other post-translational modifications. This is the first report of an isolated C2-domain causing cell proliferation inhibition and apoptosis in HEK-293 cells. Further experiments on the biochemical, mutational, localization and structural studies are needed to investigate the mechanism and functional significance of TPIP-C2 in cell proliferation regulation and apoptosis under natural conditions. We propose that if appropriately regulated, the C2-domain of TPIP-C2 cDNA can be exploited for causing cell proliferation inhibition and inducing apoptosis in human cancer cells and tissues.

Acknowledgments The authors acknowledge and thank Dr. D.J. Tindall, Dept. of Urology Research, Mayo Clinic, Minnesota for pCMV-PTEN plasmid, Dr. Rafael Pulido, Centro de Investigación Príncipe Felipe Avda, Spain for PTEN-specific monoclonal antibody (mAB 425A), Dr. Niti Puri, S.L.S., J.N.U. for pEGFP-N2 plasmid, Dr. Shweta Saran, S.L.S., J.N.U. for helping in the microscopic pictures, Dr. Babita Sharma for helping in the model. The Capacity Buildup, DST-Purse and UGC-RNRC grants from the Govt. of India/Jawaharlal Nehru University to PCR and the fellowships (JRF/SRF) from CSIR to RRM and ICMR to JKC are gratefully acknowledged.

References

1. Arena S, Benvenuti S, Bardelli A (2005) Genetic analysis of the kinome and phosphatome in cancer. Cell Mol Life Sci 62: 2092–2099
2. Venter JC, Adams MD, Myers EW et al (2001) The sequence of the human genome. Science 291:1304–1351

3. Myer MP, Stolarov JP, Eng C, Li J, Wang SI, Wigler MH, Parsons R, Tonks NK (1997) P-TEN, the tumor suppressor from human chromosome 10q23, is a dual-specificity phosphatase. Proc Natl Acad Sci USA 94:9052–9057
4. Maehama T, Dixon JE (1998) The tumor suppressor, PTEN/MMAC1, dephosphorylates the lipid second messenger, phosphatidylinositol 3,4,5-triphosphate. J Biol Chem 273:13375–13378
5. Steck PA, Pershouse MA, Jasser SA, Yung WK, Lin H, Ligon AH, Langford LA, Baumgard ML, Hattier T, Davis T, Frye C, Hu R, Swedlund B, Teng DH, Tavtigian SV (1997) Identification of a candidate tumor suppressor gene, MMAC1, at chromosome 10q23.3 that is mutated in multiple advanced cancers. Nat Genet 15:352–362
6. Li L, Ernsting BR, Wishart MJ, Lohse DL, Dixon JE (1997) A family of putative tumor suppressors is structurally and functionally conserved in humans and yeast. J Biol Chem 272:29403–29406
7. Jie-Oh Lee, Yang H, Georgescu M, Cristofano AD, Maehama T, Shi Y, Dixon JE, Pandolfi P, Pavletich NP (1999) Crystal structure of the PTEN tumor suppressor: implications for its phosphoinositide phosphatase activity and membrane association. Cell 99:323–334
8. Adey NB, Huang L, Ormonde PA, Baumgard ML, Pero R, Byreddy DV, Tavtigian SV, Bartel PL (2000) Threonine phosphorylation of the MMAC1/PTEN PDZ binding domain both inhibits and stimulates PDZ binding. Cancer Res 60:35–37
9. Cully M, You H, Levine AJ, Mak TW (2006) Beyond PTEN mutations: the PI3K pathway as an integrator of multiple inputs during tumorigenesis. Nat Rev Cancer 6:184–192
10. Wang X, Jiang X (2008) PTEN: a default gate-keeping tumor suppressor with a versatile tail. Cell Res 18:807–816
11. Lee JJ, Kim BC, Park MJ, Lee YS, Kim YN, Lee BL, Lee JS (2011) PTEN status switches cell fate between premature senescence and apoptosis in glioma exposed to ionizing radiation. Cell Death Differ 18:666–677
12. Lehman JA, Waning DL, Batuello CN, Cipriano R, Kadakia MP, Mayo LD (2011) Induction of apoptotic genes by a p73-PTEN complex in response to genotoxic stress. J Biol Chem 286:36631–36640
13. Walker SM, Downes CP, Leslie NR (2001) TPIP: a novel phosphoinositide 3-phosphatase. Biochem J 360:277–283
14. Tapparel C, Reymond A, Girardet C, Guillou L, Lyle R, Lamon C, Hutter P, Antonarakis SE (2003) The TPTE gene family: cellular expression, subcellular localization and alternative splicing. Gene 323:189–199
15. Raftopoulou M, Etienne-Manneville S, Self A, Nicholls S, Hall A (2004) Regulation of cell migration by the C2 domain of the tumor suppressor PTEN. Science 303:1179–1181
16. Georgescu MM, Kirsch KH, Kaloudis P, Yang H, Pavletich NP, Hanafusa H (2000) Stabilization and productive positioning roles of the C2 domain of PTEN tumor suppressor. Cancer Res 60:7033–7038
17. Das S, Dixon JE, Cho W (2003) Membrane-binding and activation mechanism of PTEN. Proc Natl Acad Sci USA 100:7491–7496
18. Shen WH, Balajee AS, Wang J, Wu H, Eng C, Pandolfi PP, Yin Y (2007) Essential role for nuclear PTEN in maintaining chromosomal integrity. Cell 128:157–170
19. Zhang J, Grindley JC, Yin T, Jayasinghe S, He XC, Ross JT, Haug JS, Rupp D, Porter-Westpfahl KS, Wiedemann LM, Wu H, Li L (2006) PTEN maintains haematopoietic stem cells and acts in lineage choice and leukaemia prevention. Nature 441:518–522
20. Vazquez F, Ramaswamy S, Nakamura N, Sellers WR (2000) Phosphorylation of the PTEN tail regulates protein stability and function. Mol Cell Biol 20:5010–5018
21. Leslie NR, Yang X, Downes CP, Weijer CJ (2007) PtdIns(3,4,5)P3-dependent and independent roles for PTEN in the control of cell migration. Curr Biol 17:115–125
22. Meuillet EJ, Mahadevan D, Berggren M, Coon A, Powis G (2004) Thioredoxin-1 binds to the C2 domain of PTEN inhibiting PTEN's lipid phosphatase activity and membrane binding: a mechanism for the functional loss of PTEN's tumor suppressor activity. Arch Biochem Biophys 429:123–133
23. Mehenni H, Lin-Marq N, Buchet-Poyau K, Reymond A, Collart MA, Picard D, Antonarakis SE (2005) LKB1 interacts with and phosphorylates PTEN: a functional link between two proteins involved in cancer predisposing syndromes. Hum Mol Genet 14:2209–2219
24. Tang Y, Eng C (2006) PTEN autoregulates its expression by stabilization of p53 in a phosphatase-independent manner. Cancer Res 66:736–742
25. Bajaj GD (2002) Molecular cloning and characterization of human cDNAs by a simple repeat DNA probe: identification of novel candidate genes, PhD thesis, School of Life Sciences, Jawaharlal Nehru University, New Delhi
26. Dey I, Rath PC (2005) A novel rat genomic simple repeat DNA with RNA-homology shows triplex (H-DNA)-like structure and tissue-specific RNA expression. Biochem Biophys Res Commun 327:276–286
27. Maiti R, Domselaar GHV, Zhang H, Wishart DS (2004) SuperPose: a simple server for sophisticated structural superposition. Nucleic Acids Res 32:W590–W594
28. Huang H, Cheville JC, Pan Y, Roche PC, Schmidt LJ, Tindall DJ (2001) PTEN induces chemosensitivity in PTEN-mutated prostate cancer cells by suppression of Bcl-2 expression. J Biol Chem 276:38830–38836
29. Kotamraju S, Konorev EA, Joseph J, Kalyanaraman B (2000) Doxorubicin-induced apoptosis in endothelial cells and cardiomyocytes is ameliorated by nitrone spin traps and ebselen. Role of reactive oxygen and nitrogen species. J Biol Chem 275:33585–33592
30. Linding R, Russell RB, Neduva V, Gibson TJ (2003) GlobPlot: exploring protein sequences for globularity and disorder. Nucleic Acids Res 31:3701–3708
31. Odriozola L, Singh G, Hoang T, Chan AM (2007) Regulation of PTEN activity by its carboxyl-terminal autoinhibitory domain. J Biol Chem 282:23306–23315
32. Boulares AH, Yakovlev AG, Ivanova V, Stoica BA, Wang G, Iyer S, Smulson M (1999) Role of poly(ADP-ribose) polymerase (PARP) cleavage in apoptosis. Caspase 3-resistant PARP mutant increases rates of apoptosis in transfected cells. J Biol Chem 274:22932–22940
33. Mishra RR, Chaudhary JK, Bajaj GD, Rath PC (2011) A novel human TPIP splice-variant (TPIP-C2) mRNA, expressed in human and mouse tissues, strongly inhibits cell growth in HeLa cells. PLoS ONE 6(12):e28433. doi:10.1371/journal.pone.0028433
34. Rizo J, Südhof TC (1998) C2 domain, structure and function of a universal Ca^{2+}-binding domain. J Biol Chem 273:15879–15882
35. Shao C, Novakovic VA, Head JF, Seaton BA, Gilbert GE (2008) Crystal structure of lactadherin C2 domain at 1.7Å resolution with mutational and computational analyses of its membrane-binding motif. J Biol Chem 283:7230–7241
36. Gustafson S, Zbuk KM, Scacheri C, Eng C (2007) Cowden syndrome. Semin Oncol 34:428–434
37. Yeo EJ, Ryu JH, Chun YS, Cho YS, Jang IJ, Cho H, Kim J, Kim MS, Park JW (2006) YC-1 induces S cell cycle arrest and apoptosis by activating checkpoint kinases. Cancer Res 66:6345–6352
38. Gan YH, Jhang S (2009) PTEN/AKT pathway involved in histone deacetylases inhibitor induced cell growth inhibition and

apoptosis of oral squamous cell carcinoma cells. Oral Oncol 45:e150–e154
39. Lu K, Li P, Zhang M, Xing G, Li X, Zhou W, Bartlam M, Zhang L, Rao Z, He F (2011) Pivotal role of the C2 domain of the smurf1 ubiquitin ligase in substrate selection. J Biol Chem 286:16861–16870
40. Cabarcas S, Watabe K, Schramm L (2010) Inhibition of U6 snRNA Transcription by PTEN. Online J Biol Sci 10:114–125
41. Law RH, Lukoyanova N, Voskoboinik I, Caradoc-Davies TT, Baran K, Dunstone MA, D'Angelo ME, Orlover EV, Coulibaly F, Verschoor S, Browne KA, Ciccone A, Kuiper MJ, Bird PI, Trapani JA, Saibil HR, Whisstock JC (2010) The structural basis for membrane binding and pore formation by lymphocyte perforin. Nature 468:447–451